Photomicrobial Visible Light-Induced Magnetic Mass Independent Fractionation of Mercury in a Marine Microalga

By: K. Kritee, Laura C. Motta, Joel D. Blum, Martin Tsz-Ki Tsui, and John R. Reinfelder

Kritee, K.; Motta, Laura C.; Blum, Joel D.; Tsui, Martin Tsz Ki; Reinfelder, John R. Photomicrobial Visible Light-Induced Magnetic Mass Independent Fractionation of Mercury in a Marine Microalga. ACS Earth and Space Chemistry. v2 n5 (20180517): 432-440. https://doi.org/10.1021/acsearthspacechem.7b00056

Abstract:

Methylmercury (MeHg), a highly neurotoxic substance, accumulates in aquatic food webs, and is enriched in odd isotopes (i.e., ^{199}Hg and ^{201}Hg), purportedly as a result of abiotic photodegradation in surface waters. Here, we highlight the potential role of phytoplankton in the mass independent fractionation (MIF) of MeHg in marine food-webs by providing evidence of (1) degradation of intracellular MeHg and reduction of intracellular inorganic mercury (Hg(II)) in the marine microalga, *Isochrysis galbana*; (2) a large, positive MIF ($\Delta^{199}Hg_{reactant} - \Delta^{199}Hg_{product} \sim 5–10‰$) during intracellular degradation of MeHg in cells exposed to visible light with no UVB, consistent with the accumulation of odd isotope-enriched MeHg in marine food-webs; and (3) a negative MIF (−1‰) during intracellular reduction of Hg(II) in the presence of UVB light. If representative of the photochemical reactivity of MeHg in marine phytoplankton, our results indicate that algal cell-mediated demethylation of MeHg by visible light could account for 20 to 55% of the total photochemically driven demethylation in the open ocean and transparent freshwater ecosystems with deep euphotic zones. Thus, our results extend the importance of phytoplankton (and possibly other light permeable microorganisms) in mercury biogeochemistry beyond their role as accumulators of MeHg and/or reducers of Hg(II) at the base of the food chain to include MeHg degradation and MIF of Hg in sunlit layers of the ocean and other aquatic systems.

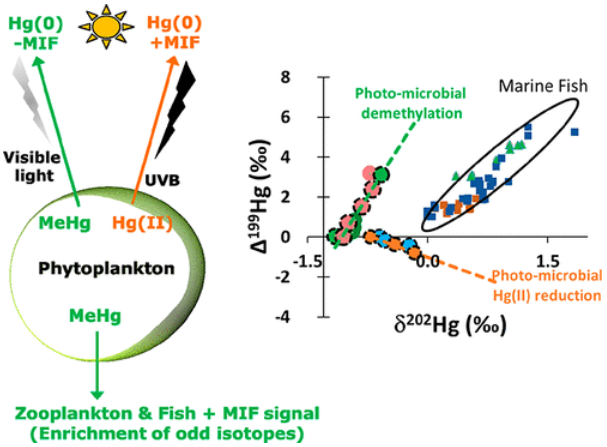

Keywords: Mercury | Stable isotope | Mass independent fractionation

Article:

Introduction

Phytoplankton play an important role in the speciation, mobility, bioaccumulation, and toxicity of Hg in aquatic ecosystems.(1−3) Although Hg methylation in the marine water column has in some cases(4−6) been correlated with phytoplankton biomass or productivity or the seasonally variable growth of pico- and nanophytoplankton (as opposed to larger (>20 μm) cells),(7) marine microalgae are not known to methylate Hg directly. They do, however, represent an important route for Hg entry into aquatic food webs.(8,9) Methylmercury, which is the most biologically available organic form of Hg, is concentrated from the dissolved phase in phytoplankton by a factor of more than 10^4 from seawater.(10,11) Cells enriched in MeHg are then consumed by zooplankton, which in turn are a primary food source of larval, juvenile, and some adult fish. Indeed, nearly all of the MeHg accumulated by zooplankton and fish is from their diet.(12−14) Two bacterial pathways that degrade MeHg, a reductive, enzyme-mediated process whose products are CH_4 and Hg(0), and (an) oxidative process(es) whose products are CO_2 and an unidentified form of inorganic Hg [ref (1) and references therein], have not been reported in phytoplankton. While the degradation of MeHg has been linked to the presence of plankton,(15,16) UV-mediated abiotic photochemical processes have been assumed to dominate MeHg degradation in the photic zone,(15,17) although the potential importance of dark microbial degradation of MeHg has also been discussed.(18)

The reduction of Hg(II) in marine surface waters has been primarily attributed to two phenomena: abiotic photochemical reactions(19) (with photochemical reduction of Hg(II) being nearly balanced by photo-oxidation of Hg(0)(20)) and dark microbial reactions associated with Hg-resistant microorganisms.(1) However, it is not clear if these two phenomena can completely explain the reduction of inorganic Hg(II) observed in growing cultures of marine phytoplankton.(21−24) In addition, although direct positive relationships between Hg(0)° concentrations and phytoplankton pigments have been observed in marine ecosystems,(25) it is not clear if phytoplankton can directly and/or intracellularly demethylate MeHg and/or reduce Hg(II) beyond their role in the production of extracellular dissolved organic matter (which may participate in abiotic photoreduction). While Hg transformations within many different lineages of bacterial cells have been explored in detail, including the recent demonstration of the reduction of intracellular Hg in a photomixotrophic bacterium,(24), the role of photomicrobial transformations (intracellular photochemical reactions) of MeHg or Hg(II) within phytoplankton cells has not been specifically examined.

Mercury stable isotope fractionation has proven to be a useful tool in constraining the potential sources and transformations of different forms of Hg in the environment.(26−28) Mercury stable isotopes display both mass dependent fractionation (MDF) and mass independent fractionation (MIF). The magnetic moments of odd isotopes of Hg and the nonmass-dependent variation in the nuclear volumes of Hg isotopes, especially ^{199}Hg and ^{201}Hg,(29−32) can lead to fractionation that does not scale according to isotope mass. Whereas MDF has been observed during both dark

transformations and photochemical reactions, MIF has not been observed during any dark microbial Hg transformations investigated to date.(33−37)

With respect to stable isotope fractionation, photomicrobial Hg transformations lie at the interface between biology and photochemistry. Stable isotope fractionation of Hg during dark microbial reduction(33−35) and also during abiotic UV-mediated processes(29−31) has been documented, but the effects of intracellular photoreduction/degradation of Hg(II) or MeHg in phytoplankton on Hg stable isotopes has not been explored.(38) A clear understanding of the Hg isotopic signatures of phytoplankton-mediated transformations, which could affect the isotopic composition of oceanic Hg(0) in addition to that of MeHg in fish, is necessary to interpret stable isotope ratios of Hg occurring as Hg(II) and MeHg both at the top of the food web (i.e., in fish) and in the water column and sediments.

We investigated the rates and Hg stable isotope signatures of photomicrobial transformations of Hg(II) and MeHg in marine phytoplankton exposed to visible light and varying levels of UV radiation by performing experiments with (1) sterile-filtered spent growth media containing extracellular exudates from cultures of *Isochrysis galbana,* a eukaryotic marine microalga of the globally important Prymnesiophyceae class; (2) actively growing monospecific cultures of *I. galbana*; and (3) cysteine or ocean water washed (nongrowing) *I. galbana* cells. The washed cell experiments were designed to test the ability of phytoplankton to transform intracellular Hg(II) and MeHg. We present our results in the context of known reaction mechanisms and expected ligand interactions inside and outside of phytoplankton cells and discuss the general implications of the new findings with respect to the current understanding of aquatic Hg biogeochemistry in the ocean and Hg isotope systematics.

Experimental Methods

Phytoplankton Cultures

Experiments were conducted using the unicellular, eukaryotic, marine microalga *Isochrysis galbana* (strain ISO, CCMP1323). *Isochrysis*is a common genus in temperate marine waters and represents the globally distributed class *Prymnesiophyceae*. Live cultures of *I. galbana* were grown in Aquil artificial seawater media(39) with 300 μM nitrate and 10 μM phosphate and were maintained at 18 °C under a 12:12 h light/dark regime with 200 μmol quanta m^{-2} s^{-1} irradiance provided by cool white fluorescent low pressure Hg lamps (see more below).

Mercury Reduction Experiments

Photochemical reduction of Hg(II) or MeHg was examined in growing whole culture, phytoplankton exudate, and washed cell experiments (see SI Tables 1 and 2 for details of all experiments). For all experiments, 100 μg/g inorganic Hg(II) and MeHg stocks were made from powdered Sigma-Aldrich mercuric nitrate monohydrate and powdered Crescent Chemical Company methylmercury chloride, respectively. For growing culture and exudate experiments, the Hg-free cultures were acclimatized to a 24 h light regime for 2 days. After this acclimatization, cultures (or the collected spent media, i.e., culture filtered through 0.2 μm polycarbonate filters) were either incubated with Hg(II) or MeHg for up to 20 h in the dark, after

which lights were turned on and reactors were purged with Hg-free air to start the reduction experiments. In growing culture experiments, both intra- and extracellular Hg was present and the kinetics and isotopic fractionation were affected by both algal exudates and the intracellular environment. For intracellular experiments, phytoplankton cells in the early exponential phase (between 4.5×10^4 and 5×10^4 cells ml^{-1}) were exposed to Hg(II) or MeHg at the beginning of a 12 h dark period and were allowed to accumulate Hg(II) or MeHg for up to 3 days. Repeated tests showed that after this accumulation period most of the added Hg(II) or MeHg was associated with the cells and the filtrate/exudate contained <2% of the added Hg. To remove extracellular Hg, cells were washed with a solution of reduced cysteine and/or synthetic ocean water (SOW) to removed surface-bound Hg.(40−42) Our data indicates that 30–40% of the Hg(II) associated with cells (in nmol/chla) after seawater wash is removed after cysteine wash (SI Table 1). As described earlier,(42) the Hg that remains associated with cell surface after cysteine washing steps is not labile. In addition, the calculation of fractionation factor does not depend on the initial isotopic composition of the reactant Hg.

Briefly, to wash the cells they were first concentrated by centrifugation (1600*g*, 3 min) and washed twice by resuspension in 20 mL of SOW. For cysteine washes, the cells were recentrifuged, and resuspended in 20 mL of 8 mM cysteine for 4 min. The cysteine wash solution was prepared fresh just prior to use in N_2-purged 50% SOW. After being washed with cysteine, cells were washed with SOW and resuspended in Aquil culture media without vitamins or trace metals. Stock phytoplankton cultures were initially axenic and all precautions were taken to exclude bacteria from experimental cultures.

All Hg reduction experiments were carried out in the laboratory at 22 to 25 °C using cool white fluorescent lamps (Philips 48″ 40 W F40T12/CWSUPREME/ALTO; see Supporting Information for details on energy emitted by the lamp and its effect on fractionation). Cells or exudates were incubated in either borosilicate glass (custom-made at University of Michigan)(33) or UV transparent Nalgene Teflon fluorinated ethylene propylene (FEP) 1 L, natural translucent narrow-mouth (381600-0032) bottles that were purged continuously with sterile (0.2 μm filtered) Hg-free air to remove Hg(0) as described earlier.(33) The concentration and Hg isotopic composition of reactant Hg(II) or MeHg remaining in each reactor was tracked over time by periodically removing 50 mL samples that were immediately weighed and preserved in 0.2% HCl and 10% BrCl (w/w) as explained earlier.(33) Our work with microbial reduction of Hg(II) in the same borosilicate reactors has shown previously that the results (i.e., fractionation factors) based on isotopic composition of the Hg remaining in the reactor versus isotopic composition of the vapor product trapped in $KMnO_4$ based oxidizing solution are similar even when there is some loss of Hg(0).(33) Because of uncertainties involved in estimating "*f*" as necessary for the Rayleigh distillation equation that is based on the vapor product as opposed to the liquid reactant remaining in the reactor, we did not trap the product Hg(0) (please see Kritee et al., 2007 and the associated Supporting Information for more details).(33) The usual $KMnO_4$ based traps do not maintain their oxidizing function over time periods longer than a few hours and our experiments ran for many days. Crucially, our previous work(33) has shown that irrespective of the efficiency of the $KMnO_4$ traps in trapping the product Hg(0), isotope data from trapped product (Hg[0]) showed no fractionation during volatilization/leakage of product from the apparatus.(33) For Teflon reactors, wall losses of Hg(II) and MeHg are not observed with seawater.(43)

We used light meters for both visible (LI-COR LI-250 PAR light meter) and UV (Sper Scientific UV Light Meter UVA/UVB-850009) to measure adsorption spectra of the two kinds of reactors. The absorption spectra of the borosilicate and Teflon bottles show that similar levels of visible (73 to 79 μmol m^{-2} s^{-1}) and UVA (∼5 μmol m^{-2} s^{-1}) light entered both kinds of reactors (Table 1). However, only about 1/3 of the UVB that entered the Teflon bottles entered the glass bottles (Table 1). In some experiments with Teflon bottles, UV radiation was blocked using Lee 226 filters, which absorb 96–100% of light below 378 nm(15,44) (Table 1). Thus, in bottles with Lee filters, cells and exudates were exposed to very little (<0.01 μmol m^{-2} s^{-1}) UVB and less than 5% of the UVA in unshielded bottles (0.2 μmol m^{-2} s^{-1}).

Table 1. Light Transmission (%*T*) and Irradiances (*E*, μmol m^{-2} s^{-1}) in Experimental Bottles[a]

	UVB (280–320 nm)		UVA (320–400 nm)		vis (400–700 nm)	
container	***%T***	***E***	***%T***	***E***	***%T***	***E***
glass	24	0.9	84	5.0	91	73
Teflon	66	2.5	82	4.9	99	79
Teflon (Lee)	0.2	<0.01	4	0.2	79	63

[a] Values do not include light attenuation due to phytoplankton (see text).

The attenuation of light due to phytoplankton was estimated using measured light absorption of *I. galbana* cultures averaged over the wavelength ranges for UVB (280–300 nm), UVA (320–400 nm), and visible (400– 700 nm) light. Culture absorbances were extended to the center of reactor Teflon bottles (5 cm) and converted to percent transmission. On the basis of these measurements, the average light attenuation due to phytoplankton was estimated as 25% of incident UVB, 20% of incident UVA, and 17% of incident visible light. For the custom-made borosilicate glass reactors that were in the shape of Erlenmeyer flasks, we estimated an average depth to center from the side and bottom of 6.5 cm (7.5 cm from the bottom, 5.5 cm from the side). For glass reactors, the average attenuation of light due to phytoplankton was therefore 31% of incident UVB, 25% of incident UVA, and 22% of incident visible light.

Mercury Concentration and Isotope Analysis

The total Hg concentrations were analyzed using a Nippon Instruments MA-2000 Hg analyzer (detection limit ∼3.5 ppt and quantification limit of <6 ppt) at the University of Michigan. All samples were pretreated and transferred to $KMnO_4$ matrix,(45) and standard solutions of NIST-3133 were used for calibration curve. We also used an in-house secondary calibration standard for checking recoveries.

Mercury isotope ratios were also analyzed at the University of Michigan using a Nu Instruments multiple collector inductively coupled plasma mass spectrometer (MC-ICP-MS) according to our previously published protocols.(46) Nomenclature for Hg isotopic compositions has been explained earlier.(38) Bracketing standards (NIST 3133) were diluted in a neutralized $KMnO_4$–H_2SO_4 matrix and concentration matched within 5%. Blanks of the same $KMnO_4$–H_2SO_4 solution were additionally employed to perform on-peak-zero measurements before the standard and sample analysis and subtracted from the analyte signals during data processing. Prior to introduction into the mass spectrometer, samples were reduced online with 2% (w/w) tin chloride and Hg(0) was liberated from solution using a custom built gas–liquid phase separator. Multiple

preparations of UM-Almáden were used to characterize instrumental performance (internal precision) (see SI Table 5). Replicate analysis of our reactor samples could not be performed in this study because of much lower concentration of Hg in the reactor and the need to reduce the entire sample for measurement of one isotopic analysis on MC-ICP-MS. In general, replicate analysis of liquid samples in $KMnO_4$ matrix after pretreatment and secondary trapping had external precision (2SD) of <0.1‰ for both Δ^{199}Hg and δ^{202}Hg.(45,47)

Differences in isotopic composition between reactant and instantaneous product at any given time during the course of a reaction were quantified as isotopic enrichment factors (ε) in units of ‰. Isotopic enrichment caused by MDF ($\varepsilon^{202}Hg_{reactant/product}$) was quantified as the slope of observed linear relationships between $\delta^{202}Hg_{reactant}$ and ln(*f*), where *f* is the fraction of initial added Hg remaining in each incubation. Isotopic enrichment due to MIF ($\Delta^{199}Hg_{reactant} - \Delta^{199}Hg_{product}$) was quantified from the slope of Δ^{199}Hg–ln(*f*) relationships. Enrichment factors are related to fractionation factors ($\alpha = R_{reactant}/R_{product}$) by the relationship ε (in units of ‰) = (α −1) × 1000. The starting isotopic composition of our MeHg stock is lighter than the standards used during isotopic analysis but this does not impact the calculation of fractionation/enrichment factor. The presentation of Rayleigh plots and all subsequent calculations normalize for the starting isotopic composition of the reactant.

Results and Discussion

Kinetics of Photomicrobial Transformations of Mercury

Reduction/degradation of Hg(II) or MeHg by *I. galbana* cells in the dark was within experimental uncertainty for at least 16 h (Figure 1A) and 28 h (data not shown), respectively. In accordance with previous research that has demonstrated Hg(II) reduction in the presence of DOC and UVB radiation,(29,30) reduction of Hg(II) species in the presence of marine algal exudates, which consist of a complex mixture of DOC molecules,(48−50) was observed with a very strong positive effect of UVB radiation on reduction rate of Hg(II) (first order rate constant (*k*) = 2.4 d^{-1} with high UVB versus 0.06–0.10 d^{-1} with low UVB; SI Tables 1 and 3). A similar dependence of the rate of Hg reduction on UVB was seen in experiments with live and growing cells that included both extracellular as well as intracellular DOC and Hg(II) (*k* = 0.43 d^{-1} versus 0.07 d^{-1}) or MeHg (*k* = 0.43 d^{-1} versus 0.02 d^{-1}) in Teflon versus borosilicate glass reactors (SI Tables 1 and 2).

Most importantly, we observed the direct reduction/degradation of intracellular Hg in the marine microalga *I. galbana*(SI Tables 1–4 and Figure 1). For the intracellular experiments, where cells were washed with cysteine (for Hg(II) exposures) or synthetic ocean water (for MeHg exposures because MeHg is mostly intracellular in phytoplankton(9) and MeHg exposed cells were sensitive to cysteine), concentrations of Hg(II) and MeHg inside the *I. galbana* cells were 0.69–1.4 and 1.1–1.3 nmol per micrograms of chlorophyll a, respectively (SI Tables 1 and 2). The reduction rate of intracellular Hg(II) (cysteine-washed cells) was 1.8–3-fold faster than that of Hg(II) in cells washed only with synthetic ocean water (*k* = 0.15–0.21 d^{-1} vs 0.38–0.47 d^{-1}) suggesting that surface-bound Hg(II) is not as efficiently reduced as intracellular Hg(II) (SI Table 1). The degradation of intracellular MeHg (SI Table 2; *k* = 0.09 vs 0.14 day^{-1}) was

slower than the reduction of intracellular Hg(II) but showed only a modest dependence on exposure to UVB light (Figure 1B).

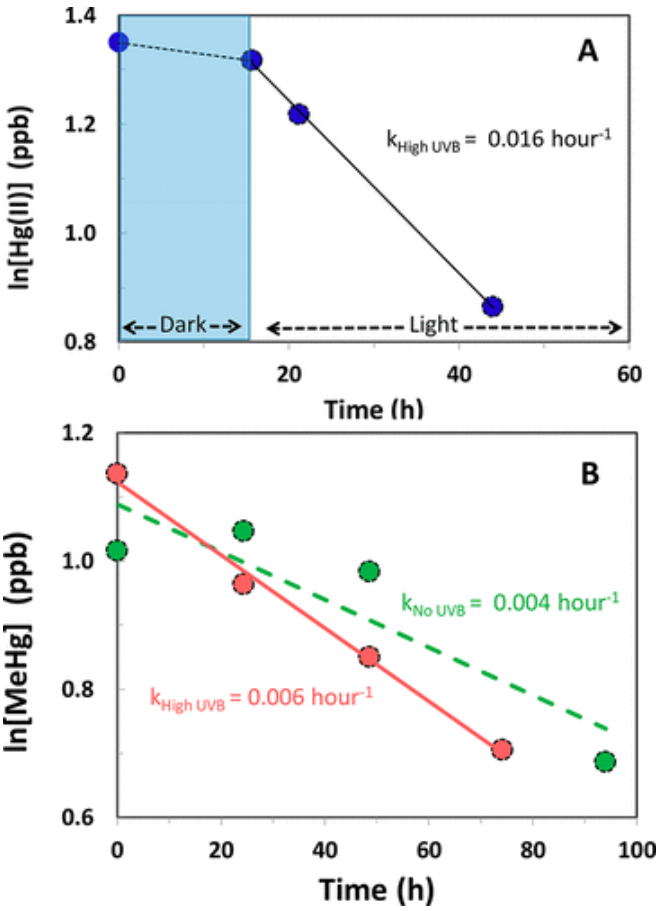

Figure 1. "Photomicrobial" reduction of Hg in the marine microalga *Isochrysis galbana*. Reduction of (A) intracellular inorganic Hg(II) in cells washed with cysteine and (B) intracellular methylmercury (MeHg) in cells washed with synthetic ocean water. For the Hg(II) experiment (A), cells were incubated in the dark for the first 16 h before being exposed to UVB in a Teflon reactor. For the MeHg experiments, cells were incubated in 12:12 light/dark cycle followed by exposure to light in Teflon reactors with (no filter, red circles) and without (Lee filter, green circles) UVB (B). Lines are best-fit models based on linear regression.

Our intracellular experiments were carried out under low irradiances and with relatively high concentrations of Hg(II) and MeHg inside *I. galbana* cells (SI Tables 1 and 2) to capture the change in isotope composition of reactant Hg species at the lowest possible concentrations required for precise isotope analysis, as is necessary in experimental studies of Hg isotope fractionation during microbial and photochemical transformations.(29,38) Although the rate constants for photomicrobial intracellular Hg(II) reduction that we observed (0.4–0.5 d^{-1}, SI Table 1) are much lower than those for photochemical reduction observed in coastal marine surface waters (4–58 d^{-1}),(18,44,51) they are an order of magnitude greater than that reported for dark biotic reduction of Hg(II) (0.03).(21,44) In addition, our rate constants for the photomicrobial degradation of intracellular MeHg (0.09–0.14 d^{-1}, SI Table 2) are comparable to those for MeHg degradation in unfiltered estuarine and coastal marine waters (k = 0.09 to 0.4 d^{-}

^{1})(18) as well as that in a clear water lake (0.17 d^{-1}) with more than six times the visible light than in our experiments.(15)

Mass Dependent Fractionation during Transformations of Intracellular Hg

Photochemical reduction of intracellular Hg(II) and MeHg resulted in positive MDF (higher δ^{202}Hg values in the reactant) indicating a preferential degradation/reduction of molecules containing lighter isotopes of Hg(II) or MeHg (SI Tables 3 and 4). Reduction of Hg(II) incubated in the light with cell exudates, but no cells, led to a higher isotopic enrichment ($\varepsilon^{202}Hg_{reactant/product}$, see Methods, hereafter ε^{202}Hg, of 1.1–1.5‰) compared to intracellular (ε^{202}Hg = 0.7–0.8 ‰) or growing algae experiments (ε^{202}Hg = 0.1–0.6‰) (SI Table 1). Reduction of Hg(II) bound to serine (N containing ligand) leads to higher MDF than Hg(II) bound to cysteine (S containing ligand);(31) it is plausible that in intracellular and growing algae experiments, Hg(II) is primarily associated with thiol (−SH) groups that protect the cell from oxidative damage. However, in experiments with cellular exudates, many other nonsulfur ligands bind to Hg(II).

Intracellular degradation of MeHg caused significant MDF (ε^{202}Hg = 0.9–1.7‰) both with and without UV light (SI Figure 1 and SI Table 2). Whereas previous research showed that abiotic photodegradation of MeHg in the presence of UV light resulted in a high extent of MDF (with ε^{202}Hg = 1.4–1.6‰),(29) in our experiments abiotic reduction of MeHg (with algal exudates or in filtered synthetic ocean water) in the absence of UV radiation caused very little MDF (ε^{202}Hg < 0.1‰). The fact that abiotic demethylation controls under low UVB conditions did not show much MDF (or any MIF, see below) is likely because in absence of intracellular processes that are activated by PAR, low UVB treatments are not able to generate radical pairs necessary for magnetic isotope effect. Overall, in our study, the photomicrobial reduction of intracellular MeHg resulted in higher MDF than abiotic photochemical reduction of extracellular MeHg in the absence of UV light. There is no clear effect of kinetics since intracellular degradation of MeHg was slightly faster than the abiotic reaction (SI Table 2). While detailed studies of the mechanisms of intracellular and abiotic MeHg degradation are needed to explain this difference, it is clear that the transformation within live phytoplankton cells resulted in greater isotopic selectivity than the abiotic reactions.

For some MeHg experiments, temporal trends in the δ^{202}Hg of Hg remaining in the reactors was not linear when plotted as a Rayleigh distillation curve [ln R/R_0 vs ln(f)] even though changes in Δ^{199}Hg were linear (e.g., compare SI Figure 1 and Figure 3 for growing algae (low UVB); data in SI Table 4). We note that the remaining Hg analyzed for isotopic composition may have contained both Hg(II) and MeHg (the methodology for quantitatively separating Hg(II) and MeHg for isotopic analysis that is being used now(52) was not available at the time of these experiments). Therefore, the observed nonlinearity of the MDF signal may have been caused by the formation of Hg(II) during MeHg degradation and MDF during both the conversion of MeHg to Hg(II) and of Hg(II) to Hg(0). Neither Hg(II) nor MeHg would adsorb to the reactor walls given the high concentration of chloride in seawater,(43) and the presence of cell-surfaces and intracellular moieties that have high concentrations of −SH groups. Moreover, adsorption would not have caused the observed nonlinear trends (SI Figure 1). In contrast, it is likely that MIF is caused by only a single step (MeHg to Hg(II); see below).

Please see Supporting Information for more observations related to MDF during Hg(II) reduction and MeHg degradation.

Mass Independent Fractionation during Intracellular Hg Reduction

The photochemical reduction of Hg(II) by growing algae, algal exudates, and intracellular algal components led to negative MIF indicating preferential enrichment of odd-mass isotopes in the product pool (Figure 2, SI Tables 1 and 3). Of these three treatments, the highest isotopic enrichment due to MIF was observed during the photomicrobial reduction of intracellular Hg(II) ($\Delta^{199}Hg_{reactant} - \Delta^{199}Hg_{product} = -1.03$ ‰).

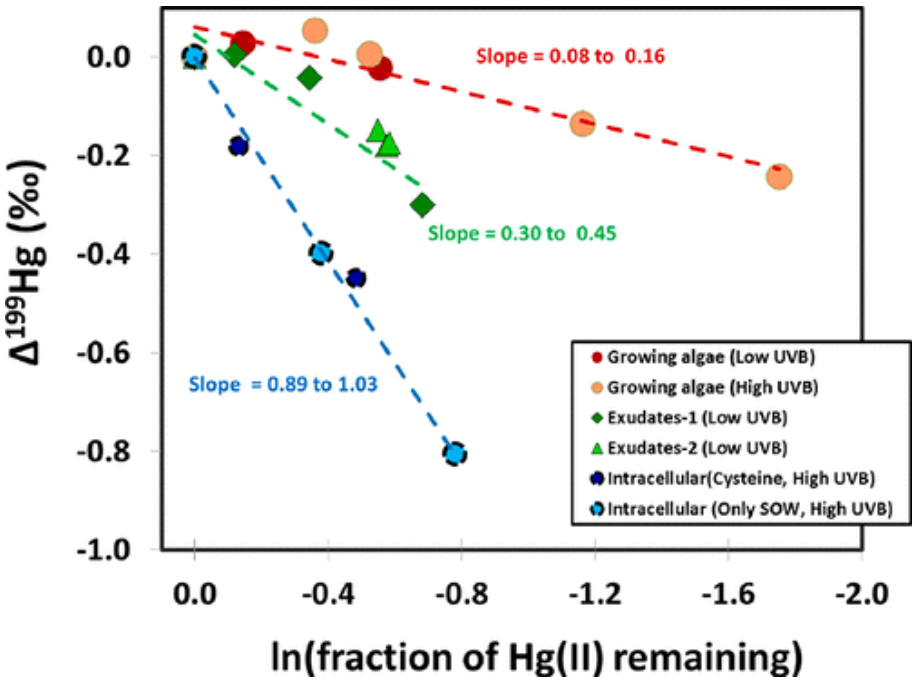

Figure 2. Negative mass independent fractionation during photomicrobial Hg(II) reduction by *Isochrysis galbana* in the presence of UV. MIF isotope enrichment factors calculated as the slopes of Δ^{199}Hg vs ln(*f*) relationships are shown for three types of Hg(II) reduction experiments: growing algae (in brown), abiotic exudates (in green), and washed cells (intracellular, in blue). No Hg(II) reduction was observed in the absence of UV light. Δ^{199}Hg values plotted on the *Y*-axis have been corrected for the nonzero starting point.

In contrast to Hg(II) reduction, photomicrobial degradation of MeHg in incubations of growing whole phytoplankton cultures and washed cells (intracellular experiments) showed positive MIF of Hg isotopes resulting in the accumulation of ^{199}Hg in the reactant pool (Figure 3, SI Tables 2 and 4). Intracellular MeHg degradation resulted in very large extents of positive MIF (Figure 3), regardless of the levels of UV light (Table 1 and Figure 3). However, MeHg degradation during abiotic control experiments (with seawater and exudates) with low levels of UV light (see Table 1, algal spent media containing exudates and abiotic synthetic ocean water) did not cause any MIF likely because low UVB treatments are not able to generate radical pairs necessary for magnetic isotope effect. Crucially, the range of high, positive MIF observed during

the photodegradation of intracellular MeHg ($\Delta^{199}Hg_{reactant} - \Delta^{199}Hg_{product}$ = 5.6‰ to 9.8‰) overlaps with results from our growing culture experiments ($\Delta^{199}Hg_{reactant} - \Delta^{199}Hg_{product}$ = 3.5‰ to 8.3‰) as well as results previously reported for abiotic photodegradation of MeHg in the presence of DOC ($\Delta^{199}Hg_{reactant} - \Delta^{199}Hg_{product}$ = 3.3 to 7.8‰)(29) (SI Table 2).

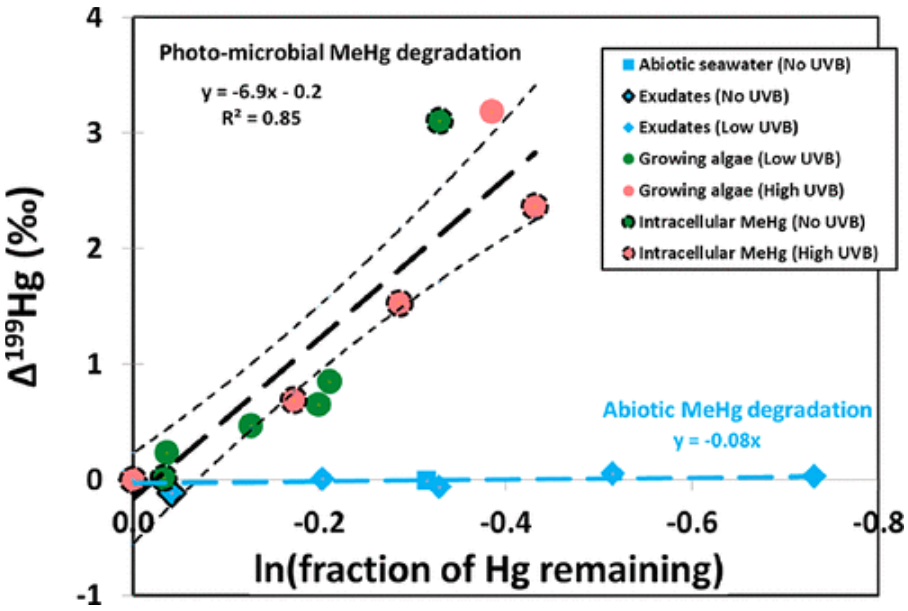

Figure 3. Mass independent fractionation during photomicrobial MeHg degradation by *Isochrysis galbana* in the presence of UV. MIF (Δ^{199}Hg vs ln(*f*)) during MeHg degradation by algae (i.e., intracellular + growing cell experiments) under conditions of no UVB (in the presence of visible light and a very limited amount of UVA) is similar to MIF in the presence of high UVB. In contrast, abiotic controls (with no or low UVB) led to negligible MIF. The dotted lines represent the lower and upper 95% confidence intervals for photomicrobial reduction. Δ^{199}Hg values plotted on the *Y*-axis have been corrected for the nonzero starting point.

Mechanism of Photomicrobial Hg Reduction and Fractionation

Our results suggest that the Hg isotopic fractionation of intracellular Hg(II) follows that of the photochemical reduction of Hg(II) bound to thiols. Both MDF (∼0.75‰) and MIF (∼−1‰) signatures generated during the photochemical reduction of intracellular Hg(II) in *I. galbana* are closer to that observed for the reduction of cysteine-bound Hg(II) (MDF of 1.3‰ and MIF of −1‰)(31) than that produced during the abiotic photochemical reduction of Hg(II) bound to serine (MDF of 1.7‰ and MIF of 3‰) or other ligands.(31) Thus, our results suggest that intracellular Hg(II) is largely complexed by thiols, which are abundant in phytoplankton cells(53−55) and that all prokaryotic and eukaryotic microbial cells containing Hg(II) are potential sources of ^{199}Hg and ^{201}Hg-enriched Hg(0) when exposed to UV light. Although we cannot identify the exact cause of the low extent of MIF of Hg(II) in the growing cells experiment, it is possible that a combination of positive and negative MIF contributed to the net isotope fractionation observed in this treatment, which contained Hg bound to exudates, cell surfaces, and intracellular ligands. It has been established that reduction of Hg(II) bound to ligands containing −SH groups causes negative MIF (enrichment of odd isotopes in product) and reduction of Hg(II) bound to N or O containing ligands causes positive MIF (enrichment of odd

isotopes in remaining reactant).(31) Regardless of the differences among treatments, net MIF in all experiments with Hg(II) was negative and the highest magnitude of negative MIF was observed during the reduction of Hg(II) in the "intracellular" treatment.

It seems likely that different reaction mechanisms drive photomicrobial reduction of intracellular Hg(II) and MeHg. Comparable Hg(II) reduction and MeHg degradation experiments carried out under similar growing cell conditions (similar cell densities and irradiances) in borosilicate glass reactors (i.e., with low UVB radiation, Table 1) show that while MeHg underwent reduction with positive MIF ($\Delta^{199}Hg_{reactant} - \Delta^{199}Hg_{product} = 3.5‰$), Hg(II) reduction in glass reactors resulted in very low negative MIF ($\Delta^{199}Hg_{reactant} - \Delta^{199}Hg_{product} = -0.08‰$). The very small extent of MIF during the reduction of Hg(II) in these experiments may have resulted from the low level of UVA and UVB or the speciation of intra- and/or extracellular Hg(II). Longer outdoor experiments are impractical but we note that abiotic outdoor experiments (in natural sunlight) with Hg(II) bound to cysteine did not lead to any Hg(II) reduction in the absence of UV light (Teflon + UV–B Lee filter) for ~11 h (both starting and ending concentrations were 40 ppb).

Our results show large extents of positive MIF and low $\Delta^{199}Hg/\Delta^{201}Hg$ ratios (~1 for Hg(II), SI Figure 2; ~1.2 for MeHg, SI Figure 3), indicative of the magnetic isotope effect (MIE). We note that our data provide no support for MIF due to UV self-shielding (SI Tables 3–4 and SI Figure 2) or nuclear volume effect. Large extents of MIF, that occur during abiotic photochemical transformations of Hg(II) and MeHg bound to organic ligands with O, N, or S functional groups, have been ascribed to the magnetic isotope effect (MIE)(29,31) which leads to a $\Delta^{199}Hg/\Delta^{201}Hg$ ratio of 1.0 for Hg(II) and 1.2 to 1.3 for MeHg, which is in contrast to a higher value of 1.6 for the nuclear volume effect.(32) The pathway leading to this magnetic MIF has been proposed to be UV driven generation of radical pairs, which leads to spin interconversion mediated by hyperfine coupling. Our results (see SI Figures 2 and 3) support the conclusion that the fundamental pathway responsible for MIF in our experiments is magnetic MIF.

Possible Routes for Generation of Radical Pairs

The pathway leading to MIE during abiotic photochemical reactions (e.g., Bergquist and Blum, 2007) has been proposed to be UV driven generation of radical pairs (which leads to spin interconversion mediated by hyperfine coupling).(29,31) To the best of our current understanding, generation of radical pairs is necessary for magnetic isotope effect. While the exact pathway to generation of radical pairs in our intracellular demethylation experiments is not clear at this time (see two options below), involvement of MIE during the photomicrobial reduction of intracellular MeHg provides evidence for the generation of radical pairs in the presence of visible light and very low intensities of UVA (i.e., in absence of significant UV). We can not rule out extracellular demethylation of MeHg (that remains associated with cell surface after seawater wash(56)). However, given the seawater vs intracellular environment, we expect intracellular (soluble) MeHg to be more reactive than membrane-bound MeHg.

So how are these radical pairs generated inside cells? Singlet oxygen has been shown to be the likely reductant in the UV-mediated abiotic demethylation of MeHg.(57) While the photosynthetic apparatus of algae can generate singlet oxygen with photosynthetically active radiation (PAR, i.e., visible light) and without UV;(58) it is unclear if, or how, singlet oxygen

can lead to generation of radical pairs that are necessary for MIE. Another possibility is that the intracellular radicals(59) and radical pairs(58) generated in phytoplankton cells due to oxidative damage lead to MIE.

Photomicrobial Contribution to the MIF Signature of Hg in Fish and MeHg Degradation in Marine Surface Waters

Photomicrobial reduction of intracellular Hg(II) in the presence of UV radiation, which produces negative MIF in the reactant pool (Figure 2, SI Tables 1 and 3), could not contribute to the positive MIF signature of Hg widely observed in fish.(26,28,29) Moreover, and in contrast to MeHg, Hg(II) accumulated by phytoplankton is poorly assimilated by grazers(9) and thus is not efficiently transferred to fish (Hall et al., 1997).(12) Experimental caveats notwithstanding (see above), based on our rate constants for the photochemical reduction of intracellular Hg(II) scaled to 12 h of daylight ($\sim$0.2 d^{-1}), the average concentration of inorganic Hg(II) in suspended particles in the ocean (40 fM),(20) and assuming that 9% of particulate Hg(II) is intracellular,(9) we estimate that photomicrobial reduction of intracellular Hg(II) could account for a global annual Hg reduction rate of $\sim$5 Mmol y^{-1} (see SI Table 6 for calculations). This is of the same order of magnitude as the annual rate of biological reduction of Hg(II) in the mixed layer of the ocean (17 Mmol y^{-1}) and the vertical flux of Hg from the surface to deep sea by particle sinking (16 Mmol y^{-1}), as estimated by Soerensen et al.(20) Although the net Hg isotopic fractionation associated with the much larger, but nearly balanced rates of abiotic photochemical reduction and oxidation of Hg (about 1000 Mmol y^{-1} each) is uncertain, the reduction of intracellular algal Hg(II) is expected to produce Hg(0) in marine surface waters that is enriched in ^{199}Hg in excess of its mass-dependent value.

In contrast to transformations of Hg(II), the photodegradation of intracellular MeHg resulted in large extents of positive MIF in the reactant (Figure 3). Indeed, Δ^{199}Hg versus δ^{202}Hg trajectories for the photomicrobial degradation of MeHg with or without UVB light (see Table 1 for details of UV intensities) are similar to those for UV-driven, abiotic degradation of MeHg,(29) and the isotopic compositions of the primarily MeHg in both freshwater(29) and oceanic(26,27) fish (Figure 4). This result indicates that intracellular degradation of MeHg in phytoplankton in the presence of visible light (with no UVB and very low UVA) could contribute to the accumulation of odd isotope-enriched MeHg in marine consumers. Because the soluble components of phytoplankton cells are preferentially passed on to zooplankton (algal cell walls are largely egested as fecal pellets(9)) and subsequently to organisms higher up in the food web, we expect the isotopic composition of soluble MeHg in phytoplankton will be transferred to higher trophic levels as well. As shown in Figure 4, marine consumers are enriched in odd isotopes of Hg. The relative contribution of extracellular (abiotic) versus intracellular photochemical degradation of MeHg to the enrichment of odd mass isotopes of Hg in marine consumers will depend on the environmental factors that control the percentage of total MeHg associated with plankton (e.g., microbial community composition and biomass, speciation of extracellular MeHg). We suggest that intracellular processes are expected to be most important to the enrichment of odd mass isotopes in marine food webs in ecosystems with high concentrations of phytoplankton (e.g., coastal or eutrophic ecosystems); however, this process may be important in high light, oligotrophic systems with deep chlorophyll maxima as well.

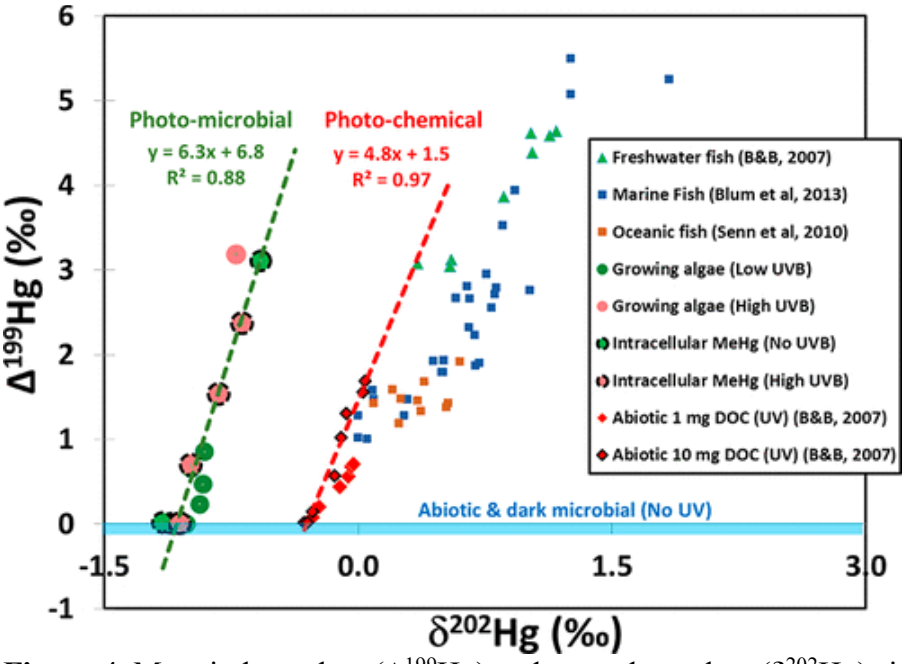

Figure 4. Mass independent (Δ^{199}Hg) and mass dependent (δ^{202}Hg) signatures in fish versus fractionation during photochemical and photomicrobial processes. A comparison of marine(26,27) and freshwater fish(29) isotopic data with stable isotopic fractionation during degradation of MeHg by photomicrobial (algal) and UV-mediated photochemical processes(29) shows that photomicrobial processes could contribute toward the accumulation of odd isotope-enriched MeHg in marine consumers. The photomicrobial and photochemical regression lines are based on all four photomicrobial demethylation experiments reported in this figure and abiotic photochemical reduction with 10 mg C/L,(29) respectively. The starting isotopic composition of MeHg stock used in our study is lighter than the standard used for isotopic analysis.

If representative of the photochemical reactivity of MeHg in marine phytoplankton generally, our results would extend the depth over which photodegradation of MeHg in natural waters can occur and the potential influence of magnetic MIF on global aquatic Hg isotope geochemistry from the UV penetrable zone (typically limited to the top 1 to 5 m) to almost the entire photic zone. For example, applying a demethylation rate constant of 0.045 d^{-1} (for 12 h of daylight), as determined for our intracellular, visible light-mediated (PAR = 63 μmol m^{-2} s^{-1}; Table 1, Teflon plus Lee, see Methods) algal demethylation experiment (SI Tables 2 and 4, Figure 3), to a phytoplankton MeHg concentration of 3 fM(17) from the sea surface to the 10% light level of the euphotic zone in the North Pacific Ocean (~54 m, average PAR ≈200 μmol m^{-2} s^{-1}),(20,60) yields a photodemethylation rate of ~5 pmol MeHg m^{-2} d^{-1} (see all assumptions in SI Table 6). On the basis of rate constants for photochemical demethylation in marine surface waters scaled to 12 h of daylight (0.04 to 0.2 d^{-1})(16,18) and the concentration of dissolved MeHg in surface waters of the North Pacific,(17) we estimate an abiotic, UV-dependent MeHg photodemethylation rate of 4–20 pmol m^{-2} d^{-1} for the upper 5 m of the ocean. Algal cell-mediated demethylation of MeHg by visible light could therefore account for 20 to 55% of the total (due to both visible and UV light) photochemically driven demethylation of MeHg in the open ocean and transparent freshwater ecosystems with deep euphotic zones. While further experiments are needed to evaluate the global applicability of the present results, if

representative of the real ocean they would extend the importance of phytoplankton (and possibly other light permeable microorganisms) in mercury biogeochemistry beyond their role as accumulators of MeHg and/or reducers of Hg(II) at the base of the food chain to include MeHg degradation and MIF of Hg in sunlit layers of the ocean and other aquatic systems.

Author Contributions

K.K., L.C.M., J.D.B., and J.R.R. conceived and designed the experiments; K.K. and L.C.M. performed the experiments; M.T.K.T. and L.C.M. performed the MC-ICP-MS runs; K.K., L.C.M., and J.R.R. analyzed the data and prepared tables; J.D.B. contributed to the interpretation of results; K.K. and J.R.R. co-wrote the paper."

The authors declare no competing financial interest.

Acknowledgments

The authors would like to thank Tamar Barkay for her involvement in the conception of this project and comments on this manuscript, Sarah Janssen for help with experiments at Rutgers and Marcus Johnson for help with stable isotopic analysis at the University of Michigan. We also thank Laura Sherman and Sae Yun Kwon for insights on various aspects of this manuscript. Funding was provided by the NSF Geobiology and Low-Temperature Geochemistry program, EAR-0952291 to J.R.R. and EAR-0952108 to J.D.B, the NSF Chemical Oceanography program, OCE-1634154 to J.R.R., and a Hatch/McIntyre-Stennis grant through the New Jersey Agricultural Experiment Station.

References

1. Lin, C.-C.; Yee, N.; Barkay, T. Microbial transformations in the mercury cycle. In *Environmental Chemistry and Toxicology of Mercury*; Liu, G., Cai, Y., O'Driscoll, N., Eds.; John Wiley & Sons, Inc., 2012; pp 155– 191. Google Scholar
2. Mason, R. P.; Choi, A. L.; Fitzgerald, W. F.; Hammerschmidt, C. R.; Lamborg, C. H.; Soerensen, A. L.; Sunderland, E. M. Mercury biogeochemical cycling in the ocean and policy implications. *Environ. Res.* **2012**, *119* (0), 101– 117, Google Scholar
3. Soerensen, A. L.; Mason, R. P.; Balcom, P. H.; Sunderland, E. M. Drivers of Surface Ocean Mercury Concentrations and Air–Sea Exchange in the West Atlantic Ocean. *Environ. Sci. Technol.* **2013**, *47* (14), 7757– 7765, Google Scholar
4. Kirk, J. L.; St. Louis, V. L.; Hintelmann, H.; Lehnherr, I.; Else, B.; Poissant, L. Methylated Mercury Species in Marine Waters of the Canadian High and Sub Arctic. *Environ. Sci. Technol.* **2008**, *42* (22), 8367– 8373, Google Scholar
5. Malcolm, E. G.; Schaefer, J. K.; Ekstrom, E. B.; Tuit, C. B.; Jayakumar, A.; Park, H.; Ward, B. B.; Morel, F. M. M. Mercury methylation in oxygen deficient zones of the oceans: No evidence for the predominance of anaerobes. *Mar. Chem.* **2010**, *122* (1–4), 11– 19, Google Scholar

6. Lehnherr, I.; St. Louis, V. L.; Hintelmann, H.; Kirk, J. L. Methylation of inorganic mercury in polar marine waters. *Nat. Geosci.* **2011**, *4* (5), 298– 302, Google Scholar

7. Heimbürger, L.-E.; Cossa, D.; Marty, J.-C.; Migon, C.; Averty, B.; Dufour, A.; Ras, J. Methyl mercury distributions in relation to the presence of nano-and picophytoplankton in an oceanic water column (Ligurian Sea, North-western Mediterranean). *Geochim. Cosmochim. Acta* **2010**, *74* (19), 5549– 5559, Google Scholar

8. Watras, C. J.; Bloom, N. S. Mercury and methylmercury, in individual zooplankton: Implications for bioaccumulation. *Limnol. Oceanogr.* **1992**, *37* (6), 1313– 1318, Google Scholar

9. Mason, R. P.; Reinfelder, J. R.; Morel, F. M. M. Uptake, Toxicity, and Trophic Transfer of Mercury in a Coastal Diatom. *Environ. Sci. Technol.* **1996**, *30* (6), 1835– 1845, Google Scholar

10. Hammerschmidt, C. R.; Finiguerra, M. B.; Weller, R. L.; Fitzgerald, W. F. Methylmercury accumulation in plankton on the continental margin of the Northwest Atlantic Ocean. *Environ. Sci. Technol.* **2013**, *47* (8), 3671– 3677, Google Scholar

11. Hammerschmidt, C. R.; Fitzgerald, W. F. Bioaccumulation and trophic transfer of methylmercury in Long Island Sound. *Arch. Environ. Contam. Toxicol.* **2006**, *51* (3), 416– 424, Google Scholar

12. Hall, B. D.; Bodaly, R. A.; Fudge, R. J. P.; Rudd, J. W. M.; Rosenberg, D. M. Food as the Dominant Pathway of Methylmercury Uptake by Fish. *Water Air Soil Pollut.* **1997**, *100* (1–2), 13– 24 Google Scholar

13. Wright, D. D.; Frazer, T. K.; Reinfelder, J. R. The influence of river plume dynamics on trace metal accumulation in calanoid copepods. *Limnol. Oceanogr.* **2010**, *55* (6), 2487– 2502, Google Scholar

14. Kehrig, H. d. A. Mercury and Plankton in Tropical Marine Ecosystems: A Review. *Oecologia Australis* **2011**, *15* (4), 869– 880, Google Scholar

15. Lehnherr, I.; St. Louis, V. L. Importance of Ultraviolet Radiation in the Photodemethylation of Methylmercury in Freshwater Ecosystems. *Environ. Sci. Technol.* **2009**, *43* (15), 5692– 5698, Google Scholar

16. Monperrus, M.; Tessier, E.; Amouroux, D.; Leynaert, A.; Huonnic, P.; Donard, O. F. X. Mercury methylation, demethylation and reduction rates in coastal and marine surface waters of the Mediterranean Sea. *Mar. Chem.* **2007**, *107* (1), 49– 63, Google Scholar

17. Hammerschmidt, C. R.; Bowman, K. L. Vertical methylmercury distribution in the subtropical North Pacific Ocean. *Mar. Chem.* **2012**, *132–133* (0), 77– 82, Google Scholar

18. Whalin, L.; Kim, E.-H.; Mason, R. Factors influencing the oxidation, reduction, methylation and demethylation of mercury species in coastal waters. *Mar. Chem.* **2007**, *107* (3), 278– 294, Google Scholar

19. Mason, R. P.; Lawson, N. M.; Sheu, G. R. Mercury in the Atlantic Ocean: factors controlling air–sea exchange of mercury and its distribution in the upper waters. *Deep Sea Res., Part II* **2001**, *48* (13), 2829– 2853, Google Scholar

20. Soerensen, A. L.; Sunderland, E. M.; Holmes, C. D.; Jacob, D. J.; Yantosca, R. M.; Skov, H.; Christensen, J. H.; Strode, S. A.; Mason, R. P. An Improved Global Model for Air-Sea Exchange of Mercury: High Concentrations over the North Atlantic. *Environ. Sci. Technol.* **2010**, *44* (22), 8574– 8580, Google Scholar

21. Mason, R. P.; Morel, F. M. M.; Hemond, H. F. The role of microorganisms in elemental mercury formation in natural waters. *Water, Air, Soil Pollut.* **1995**, *80*, 775– 787, Google Scholar

22. Lanzillotta, E.; Ceccarini, C.; Ferrara, R.; Dini, F.; Frontini, F. P.; Banchetti, R. Importance of the biogenic organic matter in photo-formation of dissolved gaseous mercury in a culture of the marine diatom Chaetoceros sp. *Sci. Total Environ.* **2004**, *318* (1–3), 211– 221, Google Scholar

23. Wu, Y.; Wang, W.-X. Intracellular speciation and transformation of inorganic mercury in marine phytoplankton. *Aquat. Toxicol.* **2014**, *148* (0), 122– 129, Google Scholar

24. Gregoire, D. S.; Poulain, A. J. A physiological role for Hg(II) during phototrophic growth. *Nat. Geosci.* **2016**, *9* (2), 121– 125, Google Scholar

25. Baeyens, W.; Leermakers, M. Elemental mercury concentrations and formation rates in the Scheldt estuary and the North Sea. *Mar. Chem.* **1998**, *60* (3–4), 257– 266, Google Scholar

26. Senn, D. B.; Chesney, E. J.; Blum, J. D.; Bank, M. S.; Maage, A.; Shine, J. P. Stable Isotope (N, C, Hg) Study of Methylmercury Sources and Trophic Transfer in the Northern Gulf of Mexico. *Environ. Sci. Technol.* **2010**, *44* (5), 1630– 1637, Google Scholar

27. Blum, J. D.; Popp, B. N.; Drazen, J. C.; Anela Choy, C.; Johnson, M. W. Methylmercury production below the mixed layer in the North Pacific Ocean. *Nat. Geosci.* **2013**, *6* (10), 879– 884, Google Scholar

28. Kwon, S. Y.; Blum, J. D.; Chen, C. Y.; Meattey, D. E.; Mason, R. P. Mercury Isotope Study of Sources and Exposure Pathways of Methylmercury in Estuarine Food Webs in the Northeastern U.S. *Environ. Sci. Technol.* **2014**, *48* (17), 10089– 10097, Google Scholar

29. Bergquist, B. A.; Blum, J. D. Mass-dependent and mass-independent fractionation of Hg isotopes by photo-reduction in aquatic systems. *Science* **2007**, *318* (5849), 417– 420, Google Scholar

30. Zheng, W.; Hintelmann, H. Mercury isotope fractionation during photoreduction in natural water is controlled by its Hg/DOC ratio. *Geochim. Cosmochim. Acta* **2009**, *73* (22), 6704– 6715, Google Scholar

31. Zheng, W.; Hintelmann, H. Isotope Fractionation of Mercury during Its Photochemical Reduction by Low-Molecular-Weight Organic Compounds. *J. Phys. Chem. A* **2010**, *114* (12), 4246– 4253, Google Scholar

32. Ghosh, S.; Schauble, E. A.; Lacrampe Couloume, G.; Blum, J. D.; Bergquist, B. A. Estimation of nuclear volume dependent fractionation of mercury isotopes in equilibrium liquid–vapor evaporation experiments. *Chem. Geol.* **2013**, *336* (0), 5– 12, Google Scholar

33. Kritee, K.; Blum, J. D.; Johnson, M. W.; Bergquist, B. A.; Barkay, T. Mercury Stable Isotope Fractionation during Reduction of Hg(II) to Hg(0) by Mercury Resistant Microorganisms. *Environ. Sci. Technol.* **2007**, *41* (6), 1889– 1895, Google Scholar

34. Kritee, K.; Barkay, T.; Blum, J. D. Mass dependent mercury stable isotope fractionation during *mer* mediated microbial degradation of monomethylmercury. *Geochim. Cosmochim. Acta* **2009**, *73* (5), 1285– 1296, Google Scholar

35. Kritee, K.; Blum, J. D.; Barkay, T. Mercury stable isotope fractionation during reduction of Hg(II) to Hg(0) by different microbial pathways. *Environ. Sci. Technol.* **2008**, *42* (24), 9171– 9177, Google Scholar

36. Rodriguez-Gonzalez, P.; Epov, V. N.; Bridou, R.; Tessier, E.; Guyoneaud, R.; Monperrus, M.; Amouroux, D. Species-Specific Stable Isotope Fractionation of Mercury during Hg(II) Methylation by an Anaerobic Bacteria (*Desulfobulbus propionicus*) under Dark Conditions. *Environ. Sci. Technol.* **2009**, *43* (24), 9183– 9188, Google Scholar

37. Perrot, V.; Bridou, R.; Pedrero, Z.; Guyoneaud, R.; Monperrus, M.; Amouroux, D. Identical Hg Isotope Mass Dependent Fractionation Signature during Methylation by Sulfate-Reducing Bacteria in Sulfate and Sulfate-Free Environment. *Environ. Sci. Technol.* **2015**, *49* (3), 1365– 1373, Google Scholar

38. Kritee, K.; Blum, J. D.; Reinfelder, J. R.; Barkay, T. Microbial stable isotope fractionation of mercury: A synthesis of present understanding and future directions. *Chem. Geol.* **2013**, *336* (0), 13– 25, Google Scholar

39. Price, N. M.; Harrison, G. I.; Hering, J. G.; Hudson, R. J.; Nirel, P. M.; Palenik, B.; Morel, F. M. Preparation and chemistry of the artificial algal culture medium Aquil. *Biol. Oceanogr.* **1989**, *6* (5–6), 443– 461 Google Scholar

40. Zhong, H.; Wang, W.-X. Controls of Dissolved Organic Matter and Chloride on Mercury Uptake by a Marine Diatom. *Environ. Sci. Technol.* **2009**, *43* (23), 8998– 9003, Google Scholar

41. Morelli, E.; Ferrara, R.; Bellini, B.; Dini, F.; Di Giuseppe, G.; Fantozzi, L. Changes in the non-protein thiol pool and production of dissolved gaseous mercury in the marine diatom Thalassiosira weissflogii under mercury exposure. *Sci. Total Environ.* **2009**, *408* (2), 286– 293, Google Scholar

42. Schaefer, J. K.; Morel, F. M. M. High methylation rates of mercury bound to cysteine by Geobacter sulfurreducens. *Nat. Geosci.* **2009**, *2* (2), 123– 126, Google Scholar

43. Parker, J. L.; Bloom, N. S. Preservation and storage techniques for low-level aqueous mercury speciation. *Sci. Total Environ.* **2005**, *337*, 253– 263, Google Scholar

44. Amyot, M.; Gill, G. A.; Morel, F. M. Production and loss of dissolved gaseous mercruy in coastal seawater. *Environ. Sci. Technol.* **1997**, *31*, 3606– 3611, Google Scholar

45. Blum, J. D.; Johnson, M. W. Recent developments in mercury stable isotope analysis. *Rev. Mineral. Geochem.* **2017**, *82* (1), 733– 757, Google Scholar

46. Blum, J. D.; Bergquist, B. A. Reporting of variations in the natural isotopic composition of mercury. *Anal. Bioanal. Chem.* **2007**, *388* (2), 353– 359, Google Scholar

47. Sherman, L. S.; Blum, J. D.; Dvonch, J. T.; Gratz, L. E.; Landis, M. S. The use of Pb, Sr, and Hg isotopes in Great Lakes precipitation as a tool for pollution source attribution. *Sci. Total Environ.* **2015**, *502*, 362– 374, Google Scholar

48. Aluwihare, L. I.; Repeta, D. J. A comparison of the chemical characteristics of oceanic DOM and extracellular DOM produced by marine algae. *Mar. Ecol.: Prog. Ser.* **1999**, *186* (186), 105– 117, Google Scholar

49. Dupont, C. L.; Ahner, B. A. Effects of copper, cadmium, and zinc on the production and exudation of thiols by *Emiliania huxleyi*. *Limnol. Oceanogr.* **2005**, *50* (2), 508– 515, Google Scholar

50. Carlson, C. A.; Hansell, D. A. DOM sources, sinks, reactivity and budgets. In *Biogeochemistry of marine dissolved organic matter*, 2nd ed.; Hansell, D. A., Carlson, C. A., Eds.; Academic Press, 2015; pp 65– 126. Google Scholar

51. Qureshi, A.; O'Driscoll, N. J.; MacLeod, M.; Neuhold, Y.-M.; Hungerbühler, K. Photoreactions of mercury in surface ocean water: gross reaction kinetics and possible pathways. *Environ. Sci. Technol.* **2010**, *44* (2), 644– 649, Google Scholar

52. Janssen, S. E.; Johnson, M. W.; Blum, J. D.; Barkay, T.; Reinfelder, J. R. Separation of monomethylmercury from estuarine sediments for mercury isotope analysis. *Chem. Geol.* **2015**, *411*, 19– 25, Google Scholar

53. Dupont, C. L.; Goepfert, T. J.; Lo, P.; Wei, L. P.; Ahner, B. A. Diurnal cycling of glutathione in marine phytoplankton: Field and culture studies. *Limnol. Oceanogr.* **2004**, *49*, 991– 996, Google Scholar

54. Satoh, M.; Hirachi, Y.; Yoshioka, A.; Kobayashi, M.; Oyama, Y. Determination of cellular levels of nonprotein thiols in phytoplankton and their correlations with susceptibility to mercury. *J. Phycol.* **2002**, *38* (5), 983– 990, Google Scholar

55. Kawakami, S. K.; Gledhill, M.; Achterberg, E. P. Production of phytochelatins and glutathione by marine phytoplankton in response to metal stress. *J. Phycol.* **2006**, *42* (5), 975– 989, Google Scholar

56. Wu, Y.; Wang, W.-X. Accumulation, subcellular distribution and toxicity of inorganic mercury and methylmercury in marine phytoplankton. *Environ. Pollut.* **2011**, *159* (10), 3097– 3105, Google Scholar

57. Zhang, T.; Hsu-Kim, H. Photolytic degradation of methylmercury enhanced by binding to natural organic ligands. *Nat. Geosci.* **2010**, *3*, 473– 476, Google Scholar

58. Liu, Y.; Edge, R.; Henbest, K.; Timmel, C. R.; Hore, P. J.; Gast, P. Magnetic field effect on singlet oxygen production in a biochemical system. *Chem. Commun.* **2005**, *2*, 174– 176, Google Scholar

59. Pinto, E.; Sigaud-kutner, T. C. S.; Leitao, M. A. S.; Okamoto, O. K.; Morse, D.; Colepicolo, P. Heavy metal induced oxidative stress in algae. *J. Phycol.* **2003**, *39* (6), 1008– 1018, Google Scholar

60. Laws, E. A.; Letelier, R. M.; Karl, D. M. Estimating the compensation irradiance in the ocean: The importance of accounting for non-photosynthetic uptake of inorganic carbon. *Deep Sea Res., Part I* **2014**, *93*, 35– 40, Google Scholar

Supporting information for "Photo-microbial visible light-induced magnetic mass independent fractionation of mercury in a marine microalga"

K. Kritee[1], Laura C. Motta, Joel D. Blum, Martin Tsz-Ki Tsui and John R. Reinfelder

This SI includes supporting text, SI Tables 1-6, SI Figures 1-3 and SI references

Supporting text

Emission spectra of cool white fluorescent lamp: Cool white fluorescent lamps produce light with sharp peaks corresponding to emissions from mercury and rare earth phosphors in the UV (312 nm, 365 nm) and visible (405 nm, 436 nm, 544 nm, 546 nm, and 611 nm), a broad peak at 485-490 nm, and several small peaks between 578 nm and 693 nm[1]. In contrast, natural sunlight consists of a continuum of finely spaced peaks of UV and visible light[2].

No effect of UV lamp expected or observed in our study: While MIF may be enhanced inside of Hg vapor compact fluorescent lamps[3], we did not observe any MIF of Hg(II) in glass reactors and Hg(II) MIF was of the opposite sign as MeHg in Teflon reactors, which indicates that the chemical form and aqueous speciation of Hg, not the light source, were the most important factors in the generation of MIF. In addition, much of the energy from the Hg vapor lamps, that cells and media were exposed to in our experiments, was concentrated in Hg emission lines at 365.4, 404.7 and 435.8 nm. All of these lines would be attenuated according to the measured spectrally resolved percent transmissions for glass, Teflon, and the Lee filter. Rose et al[4] tested the effect of different regions of the solar spectrum on the expression of MIF caused by the MIE during Hg(II) and MeHg photo-reduction. The experiments indicate that MIF produced during photo-reduction of Hg(II) is significantly influenced by both UVB and UVA radiation. They showed that for MeHg photodemethylation, however, UVB radiation is primarily responsible for the MIF with only minor contributions from UVA. To create their "no UV" experimental conditions in the reactors, Rose et al (2015) covered their reactors with acrylic sheets such that 96% and 98% of incident UV-B and UV-A, respectively, were blocked. Given that incident UV-B was ~2.5 W m^{-2} and UV-A was ~50 W m^{-2} (see Figure 1C and 1D in Rose et al), the power experienced by the contents of the reactor was ~0.1 W m^{-2} for UV-B and ~1 W m^{-2} for UV-A. If all of the UV-A was from wavelength 365.4 nm, it would translate to >3 µmol m^{-2} s^{-1}. In our no UVB (visible plus very low UV-A) experiments, UV-A irradiance was 0.2 µmol m^{-2} s^{-1}, 15 times lower than UVA intensity in the Rose et al experiments.

Mass dependent fractionation: We note that in the growing algae experiments with Hg(II) and MeHg have a fluctuating level of exposure of light because of changing number of cells in the reactor. One experiment (abiotic exudates, low UV) apparently had negative MDF with

enrichment of lighter isotopes in the reactor. This particular experiment was long (10 days), the associated Rayleigh plot had an R^2 of 0.66 and the mass dependent isotope ratios fluctuated during the experiment with significant negative MDF signal appearing only for the last data-point. Theoretically, negative (or inverse) kinetic mass dependent fractionation happens when back reactions occur (e.g., it is well documented for N stable isotopes during nitrification of nitrite to nitrate). We do not expect significant back reactions of Hg(0) in our study because we were constantly bubbling the reactors to purge out Hg(0). It is possible that some form of ionic mercury was back reacting to form MeHg.

Steps involved in mass independent fractionation during demethylation: As noted in the main text, magnetic isotope effect (MIE)[5, 6] leads to a $\Delta^{199}Hg/\Delta^{201}Hg$ ratio of 1.0 for Hg(II) and 1.2 to 1.3 for MeHg. Given that some of our $\Delta^{199}Hg/\Delta^{201}Hg$ values for our demethylation experiments (SI Table 2) are between 1 and 1.3 (instead of being between 1.2 and 1.3), a small influence of MIF during Hg(II) reduction on demethylation experiments is possible. The fact that the changes in $\Delta^{199}Hg$ for growing algae experiment with low UV for Hg(II) were not highly linear (R^2 <0.3) makes it possible that we have somehow missed seeing high negative MIF during low UVB Hg(II) reduction experiments.

SI Fig 1 MDF during MeHg Degradation

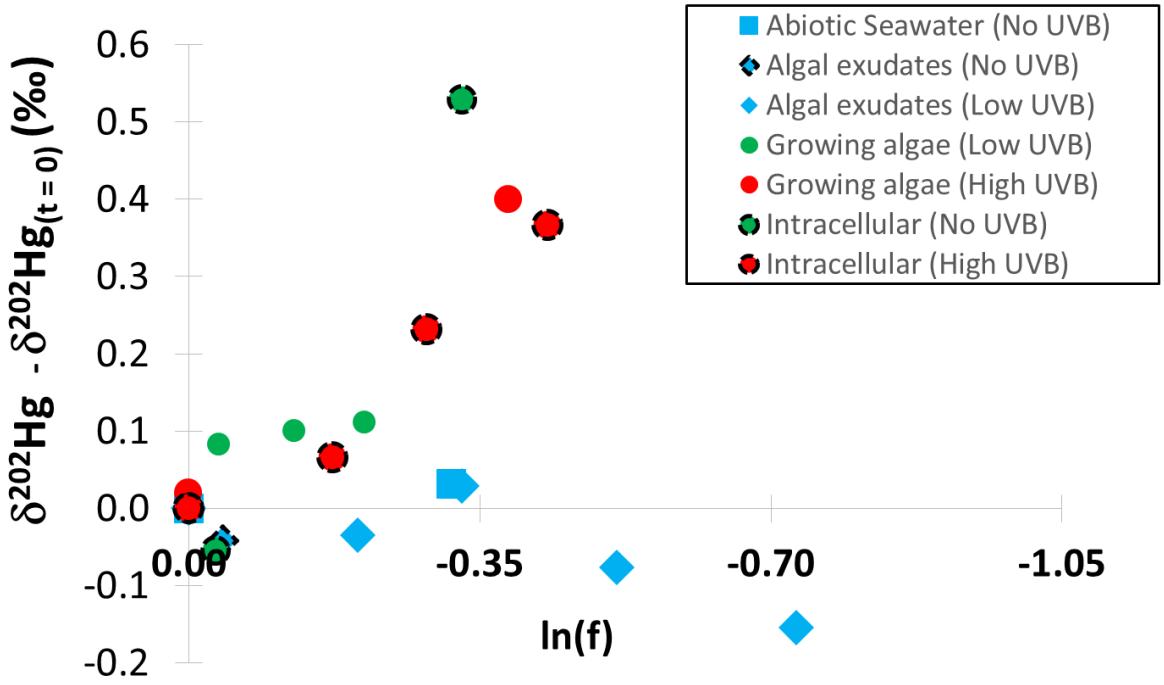

SI Fig. 2 Hg(II) reduction experiments

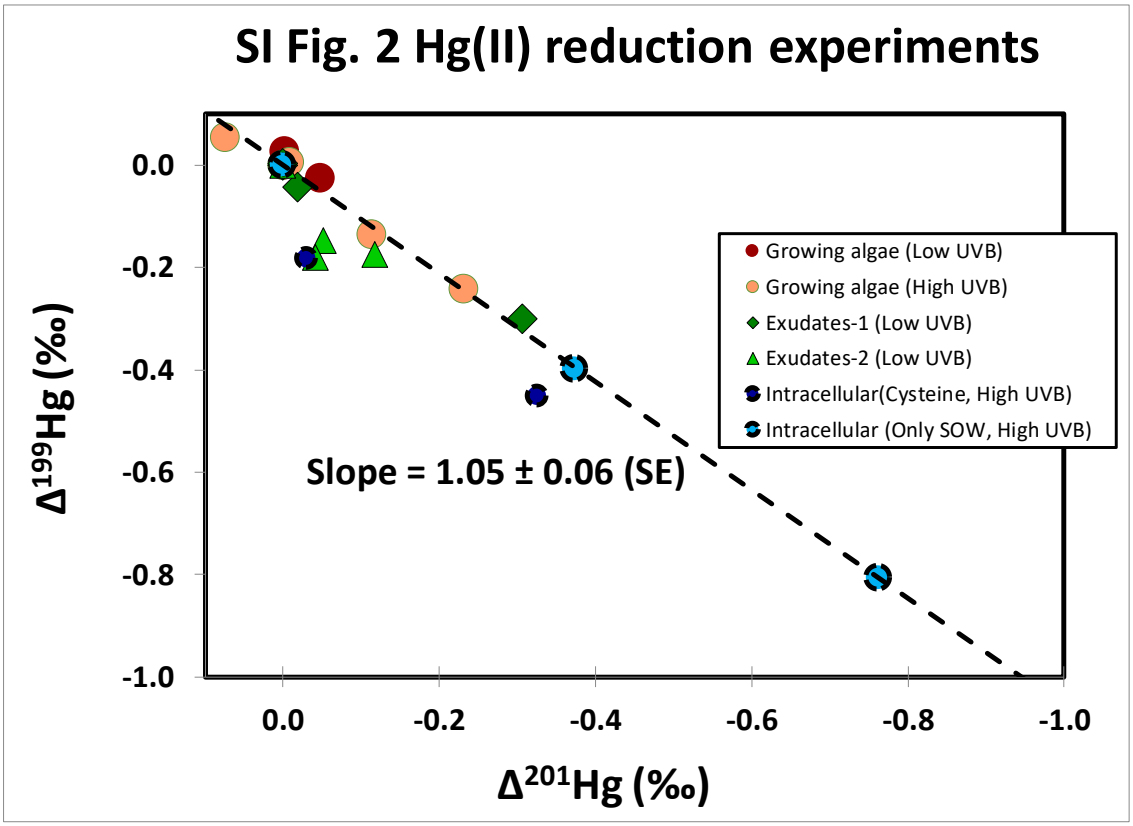

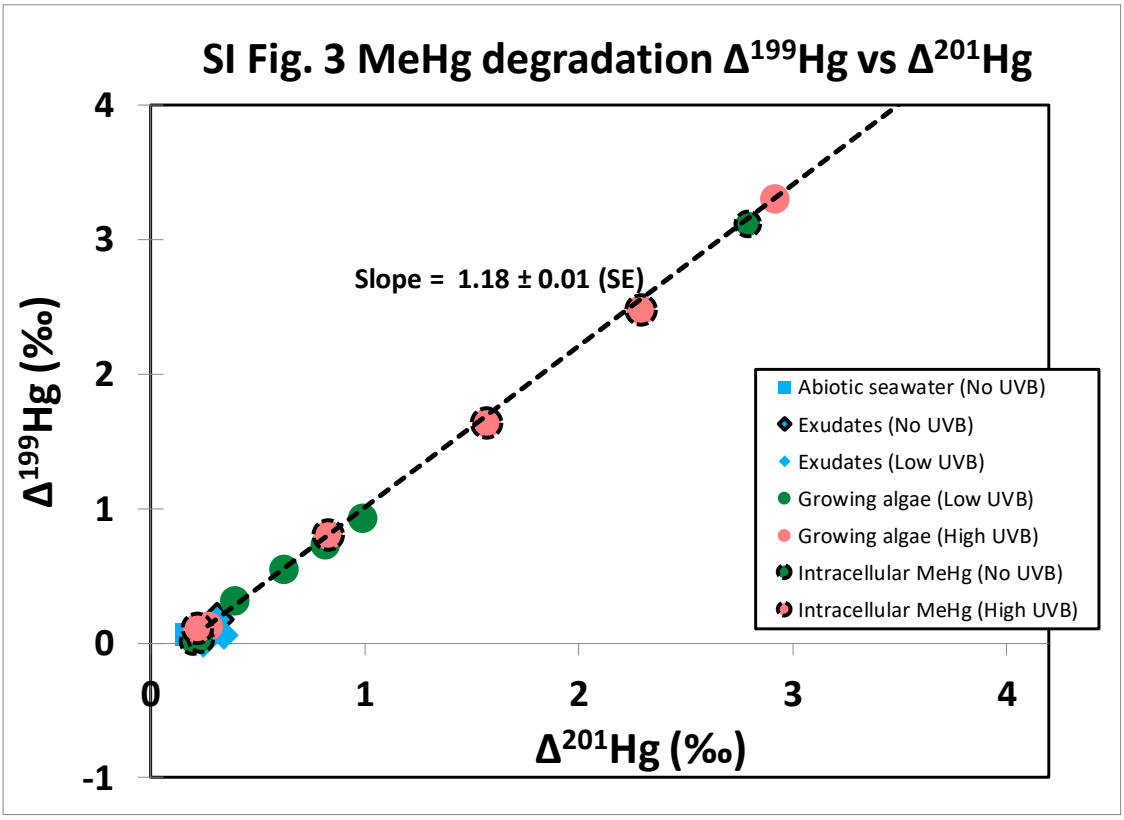
SI Fig. 3 MeHg degradation Δ199Hg vs Δ201Hg
Slope = 1.18 ± 0.01 (SE)
Δ199Hg (‰)
Δ201Hg (‰)
4
3
2
1
0
-1
0
1
2
3
4
Abiotic seawater (No UVB)
Exudates (No UVB)
Exudates (Low UVB)
Growing algae (Low UVB)
Growing algae (High UVB)
Intracellular MeHg (No UVB)
Intracellular MeHg (High UVB)

Supplementary Table 1: Summary of Hg(II) reduction experiments

Treatments	Reactor type	Initial Cells/ml	Final Cells/ml	Starting [Hg(II)] (ng/ml)	Starting [Hg(II)] (nM)	Initial intra-cellular conc. (nmol/chla)[b]	Length of experiment (days)	Rate constant ($hour^{-1}$)	Rate constant (24 hrs of light) (day^{-1})	Hg reduced by the end (%)	MDF $^{202}\varepsilon$ (‰)	MIF $^{199}\varepsilon$ (‰)	Δ199/Δ201	Δ199/δ202	Date
Abiotic marine exudates (DOC) + Hg(II) (Low UVB)	Glass[a]	5.1E+05	N/A	31.2	156	N/A	8	0.0041	0.10	50	1.08	-0.45	0.96	-0.40	April 5 2011
Abiotic marine exudates (DOC) + Hg(II) (Low UVB)	Glass[a]	5.5E+05	N/A	5.1	26	N/A	10	0.0025	0.06	44	1.47	-0.30	1.28	-0.20	Aug 23 2012
Abiotic marine exudates (DOC) + Hg(II) (High UVB)	Teflon	1.4E+06	N/A	1.1	6	N/A	4	0.1003	2.41	97	*Not analyzed for isotopes*				Jan 11 2013
Growing algae + Hg(II) (Low UVB)	Glass[a]	5.1E+05	5.1E+06	35.8	179	N/A	8	0.0031	0.07	46	0.61[c]	(-0.08)[d]	~0[e]	~0[e]	April 5 2011
Growing algae + Hg(II) (High UVB)	Teflon	4.1E+05	2.9E+05	22.1	111	N/A	4	0.0180	0.43	83	0.14[c]	-0.16	1.02	-1.07	Jan 11 2013
Intracellular Hg(II) (Cysteine wash) (High UVB)	Teflon	2.9E+05	1.2E+05	3.9	19	0.85	4	0.0159	0.38	38	0.79	-0.89	1.19	-1.11	Jan 11 2013
Intracellular Hg(II) (Cysteine wash) (High UVB)	Teflon	7.2E+05	5.7E+05	8.0	40	0.69	3	0.0195	0.47	72	*Not analyzed for isotopes*				Feb 6 2013
Intracellular Hg(II) (Ocean-water wash) (High UVB)	Teflon	2.6E+05	2.4E+05	5.8	29	1.41	4	0.0091	0.22	54	0.70	-1.03	1.06	-1.46	Jan 11 2013
Intracellular Hg(II) (Ocean-water wash) (High UVB)	Teflon	1.2E+06	6.7E+05	18.7	94	1.00	3	0.0063	0.15	15	*Not analyzed for isotopes*				Feb 6 2013

[a] *Thick Borosilicate (Also see Table 1 in the main manuscript)*

[b] *chla implies Chlorophyll a. Concentrations of intracellular contents in algal cells in often represented in units of per unit chlororphyll content*

[c] *The range of isotopic enrichments in the growing algae experiments may have resulted from the apparent lack of cell growth in the Teflon ($\delta^{202}\varepsilon = 0.1$) compared with the glass reactor ($\delta^{202}\varepsilon = 0.6$‰).*

[d] *Very poor $R^2 < 0.3$*

[e] *Because of very low MIF.*

Supplementary Table 2: Summary of MeHg degradation experiments

Treatments	Reactor type	Initial Cells/ml	Starting [Hg] (ng/ml)	Starting [Hg] (nM)	Initial intra-cellular conc. (nmol/chla)[c]	Length of experiment (days)	Rate constant ($hour^{-1}$)	Rate constant (24 hrs of light) (day^{-1})	Hg reduced by the end (%)	MDF $^{202}\varepsilon$ (‰)	MIF $^{199}\varepsilon$ (‰)	Δ199/Δ201	Δ199/δ202	Date
Abiotic marine exudates + MeHg (Low UVB)	Glass[b]	1.0E+06	10.9	55	N/A	10	0.0030	0.07	52	-0.21[f]	0	N/A	N/A	Dec 12 2012
Abiotic marine exudates + MeHg (No UVB)[a]	Teflon + Lee	2.2E+05	8.1	41	N/A	5	0.0003	0.01	0	N/A[d]	N/A[d]	N/A	N/A	Aug 17 2013
Growing Algae + MeHg (High UVB)	Teflon	7.0E+05	6.1	30	N/A	4	0.0178	0.43	73	1.2[e]	8.3[e]	1.20	8.0	Aug 27 2013
Growing algae + MeHg (Low UVB)	Glass[b]	5.6E+05	7.7	38	N/A	10	0.0010	0.02	19	0.23[f]	3.5	1.09	4.3[f]	Dec 12 2012
Intracellular MeHg (Ocean-water wash) (High UVB)	Teflon	1.5E+05	3.1	16	1.27	4	0.0057	0.14	35	0.9	5.6	1.14	6.2	Aug 26 2013
Intracellular MeHg (Ocean-water wash) (No UVB)[a]	Teflon + Lee	1.6E+05	2.8	14	1.08	4	0.0037	0.09	28	1.7	9.8	1.20	5.5	Aug 26 2013
Abiotic artificial Seawater + MeHg (No UVB)[a]	Teflon + Lee	N/A	15.4	77	N/A	5	0.0020	0.05	27	0.1	0	N/A	N/A	Aug 17 2013
Abiotic (High UVB, Low DOC, Science 2007)	Quartz	N/A	66	330	N/A	0.3	0.0313	0.75	20	1.4	3.3	1.36	2.4	
Abiotic (High UVB, High DOC, Science 2007)	Quartz	N/A	93	465	N/A	0.3	0.0321	0.77	20	1.6	7.8	1.36	4.8	

[a] *No UVB experiments also had very low UVA exposure (see Table 1)*

[b] *Thick Borosilicate (Also see Table 1 in the main manuscript)*

[c] *chla implies Chlorophyll a. Concentrations of intracellular contents in algal cells in often represented in units of per unit chlororphyll content*

[d] *Only two data points and negligible reduction*

[e] *Anomalously, there was no MDF or MIF between 0 and 54 hours. The t = 0 data point was not included in the calculation of enrichment factors*

[f] *R^2 is poor (0.66) for Abiotic marine exudates and Very poor (0.33) for growing algae (Low UV-B)*

Supplementary Table 3: Isotope data from all Hg(II) reduction experiments

Time (hrs)	[Hg] (ppb)	f (fraction Hg remaining)	δ^{202}Hg (‰)	δ^{204}Hg (‰)	δ^{201}Hg (‰)	δ^{200}Hg (‰)	δ^{199}Hg (‰)	Δ^{199}Hg (‰)	Δ^{201}Hg (‰)	Δ^{204}Hg (‰)	Δ^{200}Hg (‰)
Abiotic marine exudates (DOC) + Hg(II) (Glass: Low UVB) (April 5, 2011)											
0	31.21										
(Just after light) 20.5	31.13	1.00	-0.91	-1.36	-0.67	-0.48	-0.20	0.03	0.01	0.00	-0.03
27.5	30.01	0.96									
45.5	27.66	0.89	-0.72	-1.09	-0.53	-0.37	-0.15	0.04	0.01	-0.02	-0.01
101	22.06	0.71	-0.48	-0.63	-0.36	-0.22	-0.13	-0.01	0.00	0.08	0.02
143	18.13	0.58									
189	15.73	0.51	-0.15	-0.20	-0.41	-0.06	-0.31	-0.27	-0.29	0.02	0.02
Growing Algae + Hg(II) (Glass: Low UVB) (April 5, 2011)											
0	35.81										
(Just after light) 20.5	33.93	1.00	-0.91	-1.31	-0.68	-0.48	-0.23	0.00	0.01	0.05	-0.02
27.5	30.93	0.91									
45.5	29.36	0.87	-0.71	-1.08	-0.53	-0.32	-0.15	0.02	0.00	-0.02	0.03
101	24.63	0.73									
189	19.47	0.57	-0.54	-0.75	-0.45	-0.26	-0.16	-0.03	-0.04	0.06	0.01
Abiotic marine exudates (DOC) + Hg(II) (Glass: Low UVB) (August 23, 2012)											
(Just after light)0	5.12	1.000	-0.36	-0.52	-0.31	-0.15	-0.04	0.05	-0.05	0.01	0.03
172.9	2.96	0.578	0.40	0.62	0.20	0.20	0.00	-0.10	-0.10	0.03	0.00
220.9	2.88	0.563	0.50	0.77	0.29	0.27	-0.01	-0.13	-0.09	0.02	0.02
244.9	2.86	0.559	0.54	0.70	0.24	0.26	0.01	-0.13	-0.16	-0.10	-0.01
Abiotic marine exudates (DOC) + Hg(II) (Teflon: High UVB) (Jan 11, 2013)											
0.00	1.10										
(Just after light)15.66	0.72										
21.25	0.21	*Not analyzed for isotopic composition*									
39.22	0.06										
43.97	0.03										
Growing Algae + Hg(II) (Teflon: High UVB) (Jan 11, 2013)											
0.00	22.14		-0.54	-0.81	-0.46	-0.27	-0.16	-0.02	-0.06	0.00	0.00
(Just before light)15.6	15.45	1.00	-0.55	-0.84	-0.40	-0.26	-0.11	0.03	0.02	-0.01	0.01
21.2	13.12	0.85	-0.60	-0.82	-0.51	-0.29	-0.17	-0.02	-0.06	0.07	0.01
39.2	6.92	0.45	-0.44	-0.67	-0.50	-0.22	-0.27	-0.16	-0.17	-0.01	0.00
90.4	3.84	0.25	-0.33	-0.49	-0.53	-0.20	-0.35	-0.26	-0.29	0.00	-0.03
Intracellular Hg(II) (Cysteine + SOW washed cells; Teflon: High UVB) (Jan 11, 2013)											
0.00	3.86	1	-0.60	-0.90	-0.54	-0.30	-0.11	0.04	-0.08	0.00	0.01
(Just before light)15.7	3.73	*Not analyzed*									
21.25	3.38	0.88	-0.53	-0.80	-0.51	-0.27	-0.28	-0.14	-0.11	-0.01	-0.01
44.00	2.37	0.62	-0.23	-0.42	-0.58	-0.15	-0.47	-0.41	-0.41	-0.08	-0.03
Intracellular Hg(II) (SOW washed cells; Teflon: High UVB) (Jan 11, 2013)											
0	5.79	1	-0.71	-1.05	-0.57	-0.35	-0.16	0.02	-0.04	0.01	0.01
(Just before light) 15.9	5.32	*Not analyzed*									
39.25	3.97	0.68	-0.40	-0.69	-0.72	-0.21	-0.48	-0.38	-0.42	-0.09	-0.01
90.55	2.65	0.46	-0.16	-0.31	-0.92	-0.08	-0.83	-0.79	-0.80	-0.08	0.00
Intracellular Hg(II) (Cysteine + SOW washed cells; Teflon: High UVB) (Feb 6, 2013)											
(Just before light) 0	8.02										
15.90	4.88	*Not analyzed for isotopic composition*									
27.8	4.75										
74.0	1.79										
Intracellular Hg(II) (SOW washed cells; Teflon: High UVB) (Feb 6, 2013)											
(Just before light) 0	18.72										
15.90	17.35										
27.83	16.03	*Not analyzed for isotopic composition*									
46.25	13.32										
74.00	12.13										

Supplementary Table 4: Isotope data from all MeHg(II) reduction experiments

Time* (hrs)	[Hg] (ppb)	f (fraction Hg remaining)	δ^{202}Hg (‰)	δ^{204}Hg (‰)	δ^{201}Hg (‰)	δ^{200}Hg (‰)	δ^{199}Hg (‰)	Δ^{199}Hg (‰)	Δ^{201}Hg (‰)	Δ^{204}Hg (‰)	Δ^{200}Hg (‰)
Intracellular MeHg (Teflon with Lee Filter) No UVB and very low UVA (Aug 26, 2013)											
0.0	2.761	1.00	-1.10	-1.71	-0.83	-0.49	-0.11	0.01	0.00	-0.11	0.04
24.4	2.847	1.03									
48.7	2.672	0.97	-1.15	-1.80	-0.83	-0.64	-0.26	0.03	0.04	-0.08	-0.06
94.0	1.987	0.72	-0.57	-0.84	2.16	-0.30	2.97	3.11	2.59	0.01	-0.01
Intracellular MeHg (Teflon) High UVB (Aug 26, 2013)											
0.0	3.114	1.00	-1.05	-1.71	-0.77	-0.51	-0.15	0.11	0.02	-0.14	0.02
24.4	2.621	0.84	-0.99	-1.50	-0.11	-0.48	0.55	0.80	0.63	-0.03	0.02
48.7	2.339	0.75	-0.82	-1.31	0.75	-0.40	1.43	1.64	1.37	-0.08	0.01
74.2	2.023	0.65	-0.68	-0.88	1.58	-0.31	2.31	2.48	2.09	0.14	0.03
Growing Algae with MeHg (Teflon) High UVB (Aug 27, 2013)**											
0	6.091		-1.12	-1.69	-0.73	-0.49	-0.10	0.18	0.11	-0.02	0.07
30.8	5.744										
54.2	2.45	1.00	-1.10	-1.53	-0.76	-0.59	-0.15	0.13	0.07	0.11	-0.03
79.2	1.667	0.68	-0.72	-1.07	2.18	-0.36	3.13	3.31	2.72	0.00	0.00
Growing Algae with MeHg (Glass) Low UVB (Dec 12, 2012)											
0.0	7.69	1.00	-1.02	-1.48	-0.73	-0.55	-0.17	0.08	0.03	0.03	-0.04
81.5	7.41	0.96	-0.93	-1.41	-0.51	-0.46	0.08	0.32	0.19	-0.01	0.01
150.0	6.77	0.88	-0.92	-1.30	-0.27	-0.41	0.32	0.55	0.42	0.07	0.05
196.8	6.30	0.82	-0.98	-1.39	-0.12	-0.50	0.49	0.73	0.61	0.08	0.03
236.8	6.22	0.81	-0.91	-1.27	0.11	-0.44	0.70	0.93	0.79	0.09	0.00
Abiotic marine exudates (DOC) + MeHg (Glass) Low UVB (Dec 12, 2012)											
0.0	10.94	1.00	-0.88	-1.35	-0.59	-0.45	0.06	0.06	0.07	-0.04	-0.01
81.5	8.93	0.82	-0.91	-1.37	-0.54	-0.48	-0.17	0.06	0.14	-0.01	-0.02
150.0	7.87	0.72	-0.85	-1.35	-0.59	-0.49	-0.22	0.00	0.05	-0.09	-0.07
174.8	6.54	0.60	-0.95	-1.43	-0.68	-0.44	-0.13	0.11	0.04	0.00	0.03
236.8	5.27	0.48	-1.03	-1.55	-0.70	-0.53	-0.18	0.08	0.09	0.01	0.00
Abiotic marine exudates (DOC) + MeHg (Teflon + Lee Filter) No UVB (Aug 17, 2013)											
0	8.13	1.00	-1.10	-1.69	-0.73	-0.49	-0.10	0.18	0.11	-0.02	0.07
118.8	7.80	0.96	-1.14	-1.71	-0.81	-0.58	-0.22	0.07	0.05	-0.01	0.00
Abiotic Artificial Seawater + MeHg (Teflon + Lee Filter) No UVB (Aug 17, 2013)											
0	15.38	1.00	-1.06	-1.60	-0.83	-0.53	-0.21	0.06	-0.03	-0.02	0.00
8.3	12.76	0.83									
118.8	11.22	0.73	-1.03	-1.58	-0.75	-0.62	-0.21	0.05	0.03	-0.05	-0.10

*Light was turned on right before time = 0 minute for all experiments.

** There was no fractionation between 0 and 54 hours.

Supplementary Table 5: Isotope data for standard reference materials UM-Almáden during 2011-2013

Session date	Session Name (for internal use)	[Hg] (ppb)	Replicates	δ204	1SD	δ202	1SD	δ201	1SD	δ200	1SD	δ199	1SD	Δ204	1SD	Δ201	1SD	Δ200	1SD	Δ199	1SD
5-Apr-11	Hg_MT_Kritee_05Apr11	5.0	6	-0.90	0.06	-0.59	0.03	-0.49	0.03	-0.28	0.01	-0.16	0.06	-0.01	0.06	-0.04	0.03	0.01	0.01	-0.01	0.06
26-Apr-11	Hg_MT_Kritee_26Apr11	5.0	7	-0.80	0.06	-0.57	0.03	-0.47	0.04	-0.29	0.04	-0.17	0.04	0.05	0.05	-0.04	0.03	-0.01	0.03	-0.03	0.03
7-Jun-11	Hg_MT_Kritee_07Jun11	5.0	7	-0.89	0.09	-0.55	0.04	-0.45	0.04	-0.26	0.03	-0.16	0.03	-0.06	0.07	-0.04	0.02	0.02	0.02	-0.03	0.02
21-Jul-11	Hg_MWJ_Kritee_21Jul11	4.0	5	-0.83	0.13	-0.56	0.06	-0.47	0.11	-0.28	0.06	-0.18	0.04	0.01	0.06	-0.04	0.07	0.00	0.05	-0.03	0.02
6-Oct-11	Hg_MT_Kritee_06Oct11	4.5	7	-0.89	0.05	-0.55	0.02	-0.45	0.04	-0.28	0.04	-0.17	0.03	-0.06	0.04	-0.03	0.03	0.00	0.03	-0.03	0.03
10-Nov-11	Hg_MT_Kritee_10Nov11	5.0	5	-0.85	0.05	-0.57	0.01	-0.46	0.05	-0.27	0.03	-0.17	0.04	0.00	0.05	-0.03	0.04	0.01	0.03	-0.02	0.04
23-Feb-12	Hg_MT_Kritee7th_23Feb12	5.0	5	-0.85	0.08	-0.56	0.03	-0.43	0.04	-0.25	0.03	-0.16	0.05	-0.02	0.04	-0.01	0.03	0.03	0.02	-0.02	0.04
10-May-12	Hg_MT_Kritee8th_10May12	5.0	6	-0.90	0.10	-0.62	0.05	-0.51	0.05	-0.32	0.04	-0.19	0.03	0.03	0.04	-0.04	0.04	-0.01	0.02	-0.03	0.04
4-Jun-12	Hg_MT_HB_Kritee_Steelhead2008_04Jun12	5.0	5	-0.91	0.03	-0.61	0.03	-0.49	0.03	-0.29	0.02	-0.18	0.02	0.00	0.02	-0.03	0.03	0.01	0.02	-0.02	0.02
11-Oct-12	Hg_MT_Laura_Rutgers_23_samples_11Oct1	5.0	4	-0.82	0.10	-0.59	0.06	-0.49	0.04	-0.29	0.05	-0.15	0.06	0.06	0.03	-0.05	0.02	0.01	0.02	0.00	0.06
19-Dec-12	Hg_MT_SJ-sed._MEF-UMBS-bugs_19Dec12	5.0	5	-0.91	0.06	-0.62	0.04	-0.50	0.06	-0.31	0.05	-0.19	0.04	0.01	0.04	-0.03	0.04	0.00	0.04	-0.04	0.04
21-Jan-13	2013Jan21_MT_HgKMnO4_Rutgers	5.0	5	-0.78	0.11	-0.60	0.11	-0.50	0.13	-0.28	0.11	-0.20	0.11	0.12	0.14	-0.05	0.08	0.02	0.06	-0.05	0.09
24-Jan-13	2013Jan24_MT_HgKMnO4_Rutgers	5.0	5	-0.80	0.21	-0.48	0.10	-0.39	0.11	-0.25	0.11	-0.08	0.07	-0.08	0.24	-0.03	0.09	-0.01	0.09	0.04	0.07
25-Apr-13	2013Apr25_MT_LM_Rutgers	5.0	5	-0.86	0.05	-0.55	0.03	-0.47	0.04	-0.25	0.02	-0.14	0.02	-0.04	0.01	-0.06	0.03	0.03	0.02	0.00	0.03
22-May-13	2013May22_MT_Rutgers_Experimental_Mo	5.0	6	-0.89	0.07	-0.60	0.02	-0.48	0.04	-0.31	0.02	-0.16	0.01	0.00	0.07	-0.03	0.03	-0.01	0.02	-0.01	0.02
24-May-13	2013May22_MT_Rutgers_NJ_Sed_Janssen	5.0	7	-0.85	0.04	-0.56	0.06	-0.47	0.06	-0.28	0.04	-0.17	0.03	-0.01	0.08	-0.04	0.03	0.00	0.02	-0.03	0.02
Total Sessions				Avg	2SD	Avg	2SD	Avg	2SD	Avg	2SD	Avg	2SD	Avg	2SD	Avg	2SD	Avg	2SD	Avg	2SD
16				-0.86	0.08	-0.57	0.07	-0.47	0.06	-0.28	0.04	-0.16	0.05	0.00	0.10	-0.04	0.02	0.01	0.02	-0.02	0.04

Supplementary Table 6: Calculation of rate of photo-microbial intracellular degradation of MeHg and reduction of Hg(II)

	Rate constant (day^{-1})	[Hgp]* (pM)	Intracellular** Hg (%)	Intracellular Hg (pM)	Hg loss ($pM\ day^{-1}$)	Hg loss ($pM\ year^{-1}$)	Hg reduction rate ($pmol\ m^{-2}\ d^{-1}$)	Hg reduction rate ($nmol\ m^{-2}\ y^{-1}$)	Hg reduction rate ($Mmol\ year^{-1}$)
Intracellular Hg(II) reduction (Upper range)	0.19	0.04	9	0.0036	0.000684	0.2	36.9	13.5	**4.9**
Intracellular Hg(II) reduction (Lower range)	0.234	0.04	9	0.0036	0.0008424	0.3	45.5	16.6	**6.0**
Intracellular MeHg reduction	0.045	0.003	63	0.00189	8.439E-05	0.0	**4.6**	1.7	0.6

* Estimate of concentration of particulate Hg(II) from Soerensen et al, 2010 and particulate MeHg from Hammerschmidt and Bowman (2012)

** % of total particulate that in inside the cells (vs on the cell surface) from Mason et al (1996)

SI References

1. Elvidge, C. D.; D.M. Keith; B.T. Tuttle; Baugh, K. E., *Sensors* 2010, *10*, 3961-3988.
2. ASTM Standard Tables for Reference Solar Spectral Irradiances: Direct Normal and Hemispherical on 37° Tilted Surface G173-03. *American Society for Testing and Materials: 2012.*
3. Mead, C.; Lyons, J. R.; Johnson, T. M.; Anbar, A. D., *Environ. Sci. Technol.* 2013, *47* (6), 2542-2547.
4. Rose, C. H.; Ghosh, S.; Blum, J. D.; Bergquist, B. A., *Chem. Geol.* 2015, *405* (0), 102-111.
5. Bergquist, B. A.; Blum, J. D., *Science* 2007, *318* (5849), 417-420.
6. Zheng, W.; Hintelmann, H., *J. Phys. Chem. A* 2010, *114* (12), 4246-4253.